20th Australasian Fluid Mechanics Conference
Perth, Australia
5-8 December 2016

Two-dimensional numerical simulations of flow around a circular cylinder in oscillatory flows at low KC and Reynolds numbers

Hamidreza Eizadi, Hongwei An, Tongming Zhou, Feifei Tong

School of Civil, Environmental and Mining Engineering
University of Western Australia, Western Australia 6009, Australia

Abstract

For oscillatory flow around a circular cylinder with low Keulegan–Carpenter numbers (KC) and low Reynolds numbers (Re), totally 8 flow regimes were identified previously. Oscillatory flows with KC in the range of 4 to 6 and Re from 100 to 300 are simulated using two-dimensional (2D) numerical simulations based on OpenFOAM. The aim of this study is to examine the capability of the 2D model for capturing the boundaries of regime C in a KC-Re map. The boundaries of regime C is mapped out and compared with experimental results. The comparison shows certain level of discrepancy due to the three-dimensional nature of the flow. However, the key features of the flow agree well with the experimental observation.

Introduction

Due to close relevance to the offshore oil and gas industry, oscillatory flows around circular cylinders have been studied extensively both experimentally and numerically. Not only do the force coefficients and vortex shedding frequency but also the flow regime classification attract researchers' attention. For oscillatory flows over a circular cylinder, the hydrodynamic characteristics is governed by two non-dimensional parameters, namely the Keulegan-Carpenter number (*KC*) and the Reynolds number (*Re*), which are defined as:

$$KC = \frac{U_m T}{D} = \frac{2\pi A}{D} \tag{1}$$

and

$$Re = \frac{U_m D}{\nu}\ , \tag{2}$$

where D is the diameter of the cylinder and U_m and T are the amplitude and period of oscillation, respectively, and ν is the kinematic viscosity of the fluid. Another non-dimensional parameter, known as the Strokes number β, which is related to *KC* and *Re*, i.e. $\beta = Re/KC$, is also used in the literature. Tatsuno and Bearman (1990) conducted detailed flow visualisation for flow over an oscillating cylinder at *KC* in the range of 1.6 to 15 and Stokes number in the range of 5 to 160. The induced flow patterns were categorized into 8 different regimes. Flow Regimes A* and A are two-dimensional and symmetric to the direction of cylinder motion. In Regime A, two vortices are shed symmetrically which is absent in regime A*. Regime B is characterised with instability near the cylinder surface and pairs of contra-rotating longitudinal vortices are formed alternatively along the cylinder axis and extend in the direction of oscillation. Regimes C~G are three-dimensional. In regime C, at the beginning in the wake of the cylinder, the vortices which are shed in opposite sign from the cylinder are at the same direction of oscillation. But, after several cycles of oscillation, they push the previous ones away from the cylinder and roll up to form large vortices which are inclined to the cylinder axes. In regime D, in each half cycle of oscillation, the vortices are obliquely convected to one side of axis of oscillation and form V-shaped vortex street. In regime E, the flow is very similar to regime D except that the V-shaped vortex street switches to its mirror image frequently. A pair of vortices is seen in regime F with the opposite sign of rotation along the axis of cylinder. In regime G, the structure of flow is irregular along the cylinder axis and the transverse vortex street is seen.

Using 2D and 3D numerical simulations, Nehari et al. (2004) studied flow regimes D and F. It was found that the three-dimensionality has minor effect on the forces acting on the surface of the cylinder in the oscillation direction. Although the transversal force on the cylinder is affected by the 3D flow field, the 2D simulations validate the data from laboratory experiments. Recently, Tong et al. (2015) studied oscillatory flows around 4 circular cylinders by solving the 2D unsteady state N-S equations directly over KC and Re in the ranges of [1, 12] and [20, 200], respectively, with increment of 1 for KC and that of Re of 20. The flow regimes classified by Tatsuno and Bearman (1990) were successfully reproduced numerically. The hydrodynamic forces on the cylinder were also examined. It was found that the 2D simulation can capture regimes of C, D, E and F which are 3D. However, the regime B cannot be recognized from regimes A and A* by 2D simulation due to the similarity of cross sectional flow fields in these regimes. Therefore, the three-dimensionality of the numerical simulations has low effects on the features of different regimes and the in-line forces on the cylinder.

Although the existing work demonstrated that the 2D model can capture the key features of different flow regimes, it is still not clear if the transition between different regimes can be captured accurately, especially for the flows with 3D features. As described by Tatsuno and Bearman (1990), regime C exists only in a very small range in the tested KC-Re domain and it is surrounded by regimes A, A*, D and E. Therefore regime C is selected in this work to examine the accuracy of predicting the transition of different flow regimes using a 2D numerical model.

Numerical Setup and Mesh Dependence Check

In this paper, oscillatory flow over a circular cylinder is simulated by solving the 2D Navier-Stokes equations directly using the Open-source Field Operation and Manipulation (OpenFOAMr) C++ libraries developed by OpenCFD Ltd. The governing equations in the Cartesian coordinate system can be expressed as

$$\nabla \cdot U = 0 \tag{3}$$

and

$$\frac{\partial U}{\partial t} + (\mathrm{U}\cdot\nabla)U = -\frac{1}{\rho}\nabla p + \nu\nabla^2 U, \qquad (4)$$

where t is time, ρ is the density of the fluid, p is pressure, ν is the kinematic viscosity of the fluid and $\boldsymbol{U}$ is velocity. Figure 1 shows the rectangular computational domain (100D×100D) used in this study and the location of the circular cylinder. The domain size is proved large enough to allow the flow structures to develop in all directions. In the present study, the mesh is identical to that used by Tong et al. (2015), where mesh dependence check has been done extensively. The initial flow velocity and pressure at the domain of the cylinder are considered zero and the direction of the flow as shown in Figure 1 is horizontal and the inlet is located at the left hand side of the domain. The boundary conditions are given as follows. Flow velocity and pressure condition on the left side are given as:

$$u_x(\mathrm{t}) = U_m \sin(\omega t) \qquad (5)$$

$$\frac{\partial p(t)}{\partial x} = U_m \omega \cos(\omega t), \qquad (6)$$

where ω (≡2π/T) is the angular frequency. The velocity gradient at the direction of flow (i.e. *x*-direction) and pressure at the right boundary are set to zero. No-slip boundary condition is given on the cylinder surface.

Results and Discussion

Boundaries for Flow Regime C

The main focus of the present study is to refine the boundaries for regime C in terms of KC and Re and to verify the 2D numerical simulations. For this purpose, more than 100 cases with Re=100~300 and KC=4.0~6.0 with increment of 20 for Re and 0.1 (and 0.05 when necessary) for KC are simulated to include parts of the neighbouring regimes (Figure 2(a)). Based on the results of the time histories of lift force coefficients and the vorticity contours, the boundaries for regime C can be identified as shown in Figure 2(b). It can be seen that the refined boundaries for regime C do not match exactly with the experimental results by Tatsuno & Bearman (1990). This could be due to the 3D nature of the flow in regime C. On the other hand, some cases near the boundary lines show mixed features of regime C and the neighbouring regime. They are not counted as regime C. This could be another reason for the discrepancy shown in Figure 2(b).

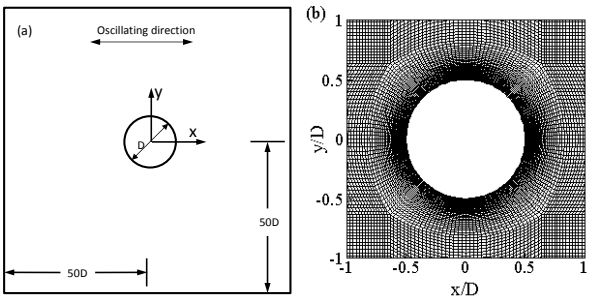

Figure 1. (a) Domain size and (b) mesh distribution around the circular cylinder in 2D numerical simulation.

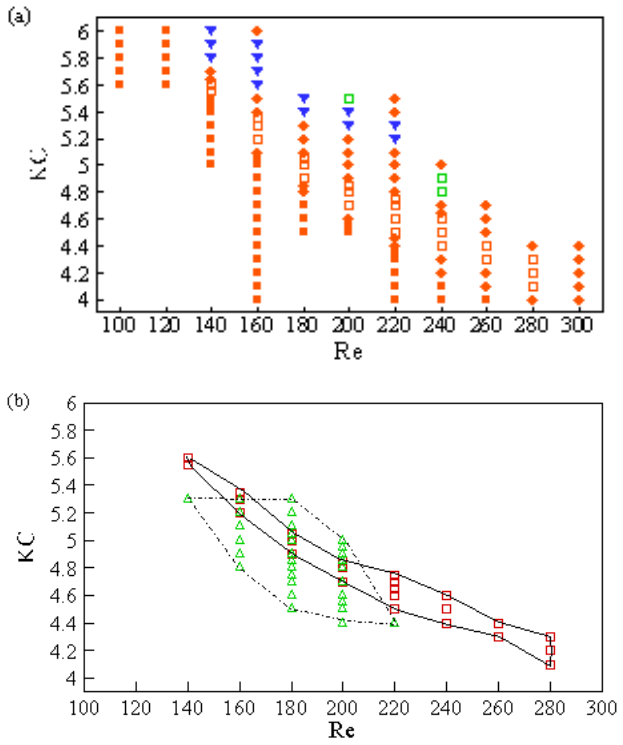

Figure 2. (a) Cases covered and the outcomes of the 2D numerical results around a circular cylinder for Regime A (■), C (□), D (▼), E (Δ) and Transitional flow (♦); (b) numerical results around a circular cylinder for regime C (□), along with the experimental results for boundaries of regime C for a circular cylinder (Tatsuno & Bearman 1990) (Δ).

Time Histories of Lift Force Coefficient

The normalized lift force (C_L) is calculated as

$$C_L = \frac{F_y}{0.5\rho D {U_m}^2} \qquad (7)$$

where F_y is the force in the *y*-direction. The time histories of the lift force coefficient for more than 200 flow periods are shown in Figure 3 to reveal the features of flow in different regimes. The corresponding key flow strcutures are given in Figure 4 through vorticity contours. For Re = 160 and KC = 4.0 (Figure 3(a)), the magnitude of the lift force coefficient C_L is very low and the flow is symmetric with respect to the *x*-axis (Figure 4(a)). These results confirm that the flow belongs to regime A. In Figure 3(b) (Re =180, KC=5.0) for regime C, a regular secondary flow period is obviously seen. The magnitude of C_L remains the same in the two halves of each secondary flow period, but with opposite sign. The secondary flow period (or quasi-flow period) is due to the flapping behaviour of the vortex street (Figure 4(b)). In Figure 3 (c) (regime D), the lift force shows strong regularity but with an obvious non-zero mean. This is because the V-shaped flow is always open towards the positive-x direction (Figure 4(c)). Figure 3(d) shows the time histories of the lift coefficient for regime E. Due to the intermittent switching of the V-shaped flow pattern (Figure 4(d)), a series of beating behaviour can be seen. However, it does not have a regular secondary flow period. C_L in Figure 3(e) shows certain features similar to regime C, such as the secondary flow period. However, the flow (Figure 4(e)) is much less regular than that shown in Figure 4(b). It is believed that this case is a transition between two different flow regimes, and it is not counted as Regime C.

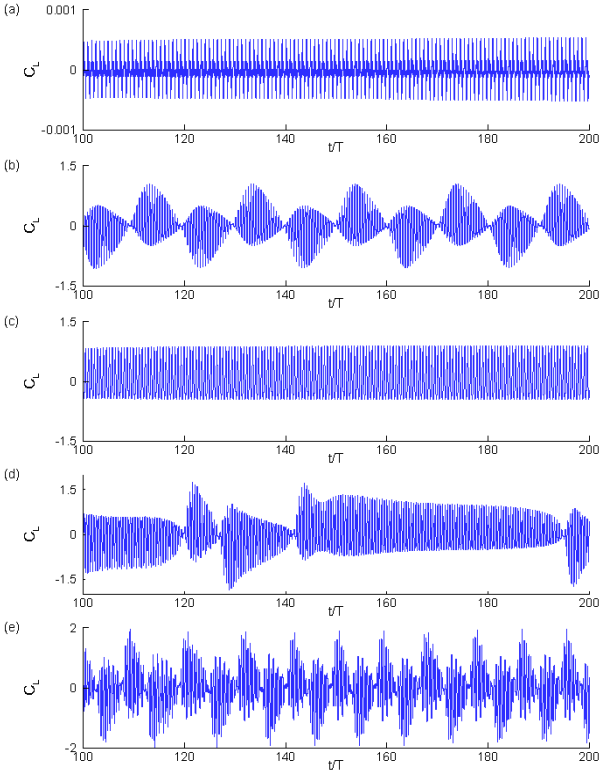

Figure 3. The time histories of lift force coefficient for different regimes. (a) Regime A (Re=160, KC=4.0), (b) Regime C (Re=180, KC=5.0), (c) Regime D (Re=140, KC=5.9), (d) Regime E (Re=240, KC=4.8), (e) Transition regime (Re=300, KC=4.4).

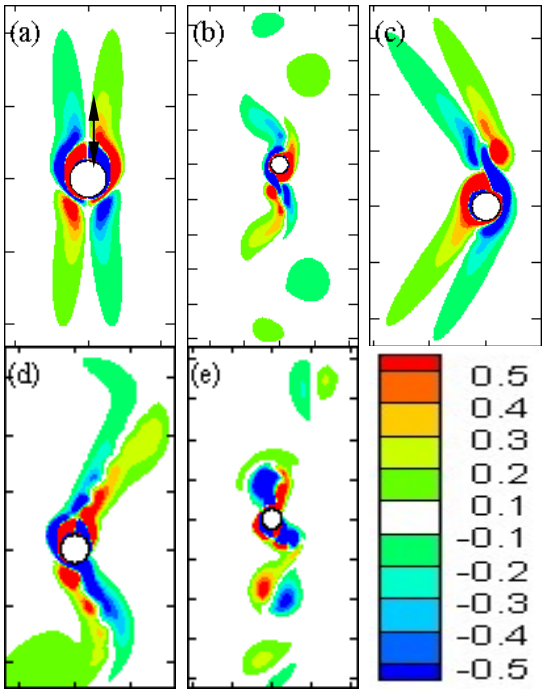

Figure 4. Vorticity contours for different regimes. (a)Regime A (Re=160, KC=4.0), (b) Regime C (Re=180, KC=5.0), (c) Regime D (Re=140, KC=5.9), (d) Regime E (Re=240, KC=4.8), (e) Transition (Re=300, KC=4.4). The cutoff level $\omega_z = \pm 1$ and the double arrow indicates the direction of oscillation.

Vortex Shedding Frequency

The frequency of the lift force is analysed here as it is closely related to vortex shedding patterns. Figure 5 shows spectra obtained by performing Fast Fourier Transform (FFT) to the measured lift force coefficient for different regimes. The *x*-axis has been normalised by the oscillating period. Figure 5(a) shows the spectrum for flow regime A with a dominating frequency identical to the frequency of the oscillatory flow. This is due to the minor flow asymmetry, but not vortex shedding. For regime C, (Figure 5(b)), it clearly shows two dominating peaks (fT=1.95 and 2.05) with very similar amplitude. A low frequency component (f_{quasi}) of 0.05 also exists, corresponding to a quasi-periodicity. A very similar behaviour has been identified by Tong et al. (2016) for a square cylinder in oscillatory flow. When the lift time history in one half of the secondary flow period (e.g. corresponding to the half period t/T = 120 ~ 130) is analysed with FFT, only one dominate frequency at fT = 1.95 can be found. The dominating frequency for lift time history in the next half of the secondary period is close to 2.05. This explains the reason for the double peaks observed in Figure 5(b). Due to the strong regularity of the lift force for flow regime D (Figure 3(c)), only one dominating peak exists in the frequency spectrum (Fig. 5(c)). For regime E, there is also only one dominating frequency although the lift force shows long period beating features. Figure 5(e) shows the spectrum of the lift force for the transitional flow. It has two peaks close to each other with a quasi-frequency. However it should be noted that the amplitudes of the double frequencies are obviously different.

The key frequency component for fT <5 is summarized in Figure 6. It can be seen that the quasi-frequency exists in all the regime C cases and the dominating frequency of the lift force can be calculated as $fT = 2 \pm f_{quasi}$. Same feature for square cylinder was reported by Tong et al. (2016).

In Figure 7, secondary flow period for Re=140~280 in regime C is summarized. It is seen that the secondary flow period reduces with the increase of the Reynolds number within the investigated range.

Conclusions

The flow field around a circular cylinder in the range of KC=4 ~6 and Re =100~300 was investigated through 2D numerical simulations. The flow regime map for regime C in the Re-KC plane was prepared. The key flow features of regime C are analysed. The main conclusions are given below.

Compared to the experimental results, the boundary lines of regime C based on the present numerical results do not match exactly with the experimental ones and this is mainly attributed to the three-dimensionality of the flow.

The lift force in regime C shows a secondary flow period due to the flapping behaviour of the vortex street.

The dominating frequency can be calculated as $fT = 2 \pm f_{quasi}T$.

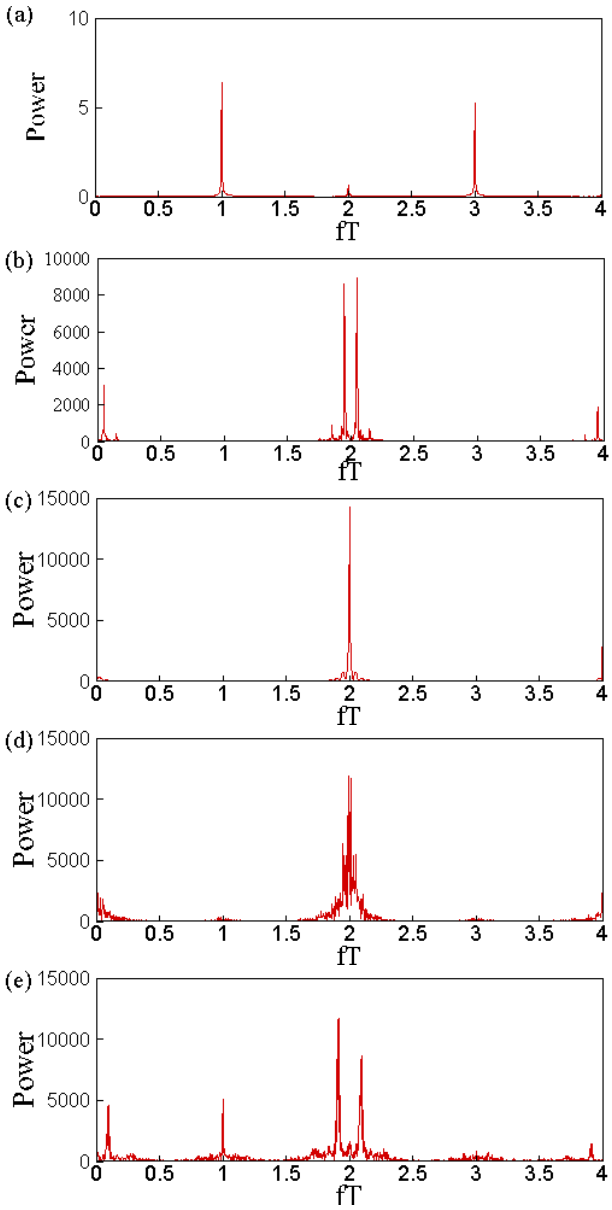

Figure 5. Spectra of the lift force coefficients for different regimes. (a) Regime A(Re=160, KC=4.0); (b) Regime C(Re=180, KC=5.0); (c) Regime D(Re=140, KC=5.9); (d) Regime E(Re=240, KC=4.8); (e) Transition(Re=300, KC=4.4).

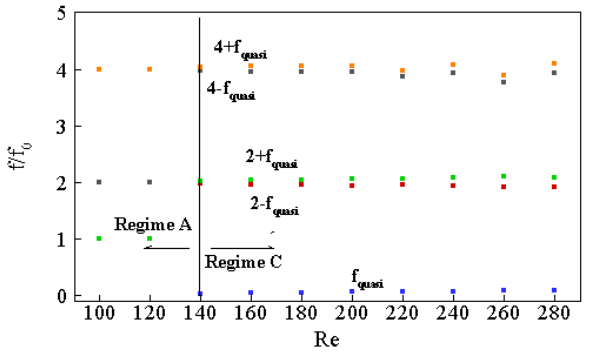

Figure 6. Quasi-periodic for six strongest frequencies on the spectrum of lift force coefficients for different Re numbers for Regime C (Re =140~280) and regime A (Re=100~120).

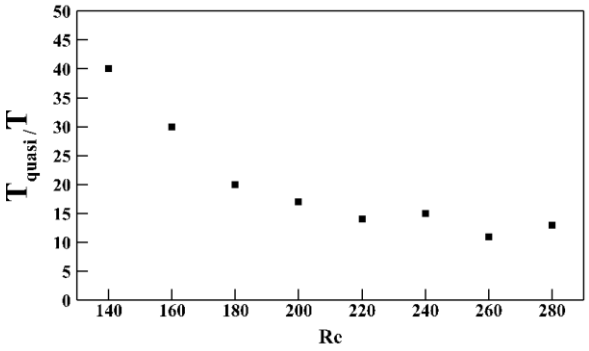

Figure 7. Ratio of the quasi-period (T quasi) to the oscillation period (T) at Re=140~280 for different KC numbers in regime C.

References

[1] An, H.W., Cheng, L. & Zhao, M., Direct numerical simulation of oscillatory flow around a circular cylinder at low Keulegan-Carpenter number. *Journal of Fluid Mechanics*, 666, 2011, 77-103

[2] Nehari, D., Armenio, V. & Ballio, F., Three-dimensional analysis of the unidirectional oscillatory ow around a circular cylinder at low Keulegan-Carpenter and beta numbers. *Journal of Fluid Mechanics*, 520, 2004, 157-186.

[3] Sumer, B.M. & Fredsøe, J., *Hydrodynamics Around Cylindrical Structures*, World Scientific, 1997.

[4] Tatsuno, M. & Bearman, P.W., A visual study of the ow around an oscillating circular cylinder at low keulegan-carpenter numbers and low stokes numbers. *Journal of Fluid Mechanics*, 211, 1990, 157-182.

[5] Tong, F.F., Cheng, L., Zhao, M. & An, H.W., Oscillatory flow regimes around four cylinders in a square arrangement under small and conditions, *Journal of Fluid Mechanics*, 769, 2015, 298-336.

[6] Tong, F.F., Cheng, L., Xiong, C., Drapper, S., & An, H.W., Lou, X., Flow regimes for a square cylinder in oscillatory flow, Submitted to *Journal of Fluid Mechanics*, 2016,